AERODYNAMIC AND HYDRODYNAMIC INTERACTIONS BETWEEN TWO YACHTS SAILING UPWIND

Alessandro Marino, Naval Architecture, Marine and Ocean Engineering, University of Strathclyde, Glasgow, UK
Francesca Tagliaferri, School of Marine Science and Technology, Newcastle University, UK
Weichao Shi, Naval Architecture, Marine and Ocean Engineering, University of Strathclyde, Glasgow, UK

During sailing yacht races, sailors struggle to keep the fastest route to the next mark and to avoid the 'shadow' of other competitors. This is in fact disadvantageous, as it creates the so-called 'dirty wind' (turbulent flow), slowing the yacht down and forcing the helm to change the route and lose pace.

Understanding the interactions between yachts is critical for racers, in order to decide the most successful tactic. The present work is focused on the investigation of a method for quantifying the interactions between two sailing yachts at both aerodynamic and hydrodynamic levels.

Two America's Cup Class (ACC) sailing yacht models are tested in the Wind Wave Current Tank and in the Towing Tank of the Hydrodynamic Laboratories at Newcastle University, UK. Three different configurations are considered, all recreating an upwind leg race scenario.

During the test, the True Wind Speed (TWS) is set constant, while the points of sail, hence the Apparent Wind Angle (AWA), the Apparent Wind Speed (AWS) and the Boat Speed (BS), change. The three investigated values of the AWA are 25°, 30° and 35°.

The aerodynamic interactions are studied by measuring the changes of the wind speed due to the presence of the models in the Tank. The models are held firm in a heeled position. The measurements show a remarkable change in the wind speed at different positions, despite the high level of turbulence that affected the measurements negatively. The hydrodynamic interactions are studied by measuring the resistance of the leeward model in the Towing Tank. The models are towed upright and heeled, simulating the same conditions as those analysed in the Wind Wave Current Tank. This is the first time that two models are tested in this kind of facility, with the aim of representing a race scenario. The measurements show that a difference in the resistance values can be appreciated when the configuration changes.

1. Introduction

Yacht races are not always won by the fastest boat. Tactics and strategy play an important role in an environment where bots' speed is mostly determined by the wind acting on the sails.
When a yacht is sailing behind another one, the sails can underperform due to the turbulence caused by the leading yacht. Even if less evident, this is true also for the water flow on hull and appendages. This can be true even at a distance and sailors know they have to avoid sailing in the shadow of another boat. However, this "danger zone" is not easy to define. This study aims to investigate a methodology to combine aerodynamic and hydrodynamic test results and thus provide data to predict the interactions between two yacht thoroughly.

1.1. Sailing yacht modelling

The dynamics of sailing yachts are largely described in literature [1], [2], [3] and their effect is studied to predict the performance of a yacht.
Broad data are available for yacht models, especially from the experiments on the Delft Systematic Yacht Hull Series (DSYHS), an extensive series of about 50 models of yacht hulls, which have been tested at the Delft University of Technology since 1970s.
These models were extensively used in a towing tank to study the resistance and the hull performance of sailing yachts in terms of hydrodynamic resistance. These datasets are used to predict a yacht's speed in given wind conditions through the use of Velocity Prediction Programmes, (VPP) [4] or to compare different possible design choices [5].
Other studies aim to build models to predict the aerodynamic forces generated by the wind on the sails [6] and provide data for a VPP.

1.2. Interactions between yachts

While the mentioned papers consider the hydrodynamic or aerodynamic forces only, some attempt have been made to combine different models and achieve an overall prediction of performance. One example is the PACT (Partnership for America's Cup Technology) prediction software [7]. It uses a Line Processing Programme (LPP), a Rig Analysis Programme (RAP), a VPP and a Race Modelling Programme (RMP) to foresee the performance of the yacht in different race scenarios, taking into account the presence of up to two yachts simultaneously.
Many studies about interactions have been carried out so far, but they mainly cover only the aerodynamics of sails. Extensive tests can be carried out in wind tunnel facilities, which involve model scale experiments. In Auckland (New Zealand) were conducted numerous works with many models, simulating race scenarios with two boats [8] or an entire fleet [9]. In both cases, the forces acting on the key model were measured in order to assess how the position of the other models affected its performance.
Aerodynamic interactions studies were performed also with the sole aid of computer simulations [10]. The authors modelled the wake of a yacht by applying a Lifting Line Method, and carried out race simulations and CFD calculations where the apparent wind felt by a yacht in a given position took into account the presence of other boats.
The knowledge about interactions between yachts is very important for the development of tools which may be used to decide the optimum strategy for a particular race.
An example is proposed by Philpott *et al*. [11], who simulate a race between two yachts. These are defined by their positions, speed and heeling angle and their performance is predicted with a VPP. A Markov chain model is applied to the wind field and the simulation is run with a fixed time increment. The weather history is used to define the condition seen by a downwind boat; equal tactics are assumed for both yachts: the choice that involves less risk is made.
Other models compare different tactics in order to define a better strategy to face a race. Having an attitude towards risk (typical of trailing boats, rather than leading ones) seems to pay off during a match race, rather than being conservative and pessimistic towards decisions such as to change one's course according to wind shifts [12].
Tools like those described above can be extremely useful for competitive sailors and implemented with weather forecasting programmes, which can record data and provide short-term forecasts about the wind behaviour [13].
When interactions between yachts are concerned, usually only the aerodynamic ones are considered, as it happens with the models described above [11] [12]. When combinations of aero- and hydrodynamic performances are available, they consider an isolated yacht only (e.g. [14]).

1.3. Paper outline

The aim of this paper is to share the lesson learned during the development of a methodology for quantifying the changes in both aero and hydrodynamic forces acting on a sailing yacht in presence of another yacht sailing in close proximity. This work is to be intended as a proof of concept: to the authors' best knowledge, there are no works in literature: about measurements performed in this kind of facilities with models at this scale of dimensions. The topic was explored with a series of experiments carried out in Newcastle University Hydrodynamics Laboratories, as part of the first author's Masters dissertation [15],. The measurements include the changes in wind velocity around the two models in a wind wave current tank and those in the hydrodynamic resistance of the downwind model in a towing tank. The latter results are obtained by recreating for the first time a race scenario with two yacht models in a towing tank.
Different configurations were tested, and different AWSs for each of them. Configurations and angles were the same in both the tanks.
An overall description of the obtained results is hereby presented, and, more importantly, of the issues faced during the development of the experimental work. The main reasons of the most unexpected results are discussed, and recommendation for future work are given.

2. Experimental method and setup

The models are tested in an upwind sailing scenario. Three configurations are tested, where the upwind model is shifted sideways, while keeping the same radial distance from the leeward one.
The aerodynamic interactions are assessed by measuring the change in the wind speed in the direction of the undisturbed flow, due to the presence of the models with two hot wires anemometers. The hydrodynamic interactions are measured in terms of the total drag of the leeward model.
All the experiments were run in the facilities of the Newcastle University Hydrodynamics Laboratories [16].

2.1. Models and facilities

Two identical Kyosho Fortune 612 III R/C models [17] are employed for the experiments described in this work. These models represent the ACC yachts used until the 32nd edition [18]. Their characteristics are as following: L_{OA}=0.612m, B=0.130m, T=0.335m, Mast height=0.83m, Δ=1.050kg. The main limitation in choosing the model was the size of the tanks, in fact, in order to test two models at once, the most suitable ones were R/C (remote control) racing ones. Among those available in commerce, the chosen ones were the best in terms of size and characteristics.

Figure 1: Sailing yacht RC model Fortune 612 [17]

The aerodynamic tests were carried out in a Wind Wave Current tank (WWC), with the following characteristics: Flume Length=11m, width=1.8m, Normal Water Depth=1m, Air Clearance=1m, Central Measurement Section=3m, Max Water Velocity=1m/s, Max wind Velocity=20m/s.
The hydrodynamic tests were carried out in a towing tank, with the following characteristics: Length=37m, Width=3.7m, Water Depth=1.25m, Normal Carriage Velocity=0-3m/s

2.2. Test configuration

Three AWAs are tested and, consequently, three Apparent Wind Speeds (AWSs) and three BSs. All the combinations are repeated for three different configurations, where the position of the upwind model is changed with respect to the leeward one, as shown in Figure 2.

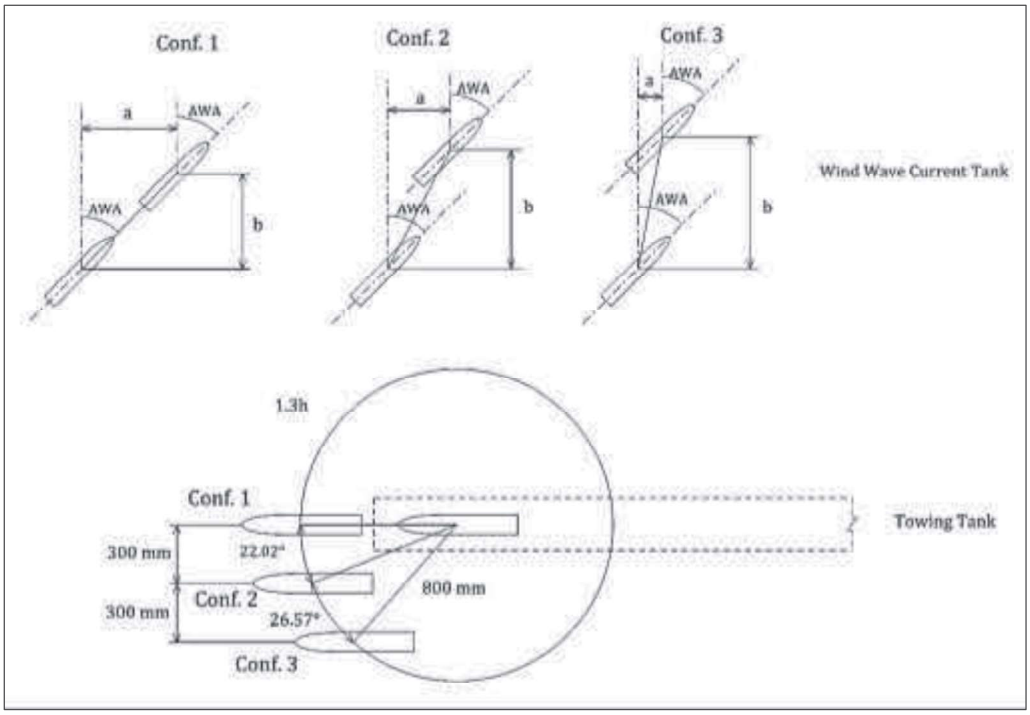

Figure 2: test configurations in Wind Wave Current Tank and Towing Tank

In Configuration 1 the models are in a straight line, regardless of the AWA; in Configuration 2 the bow of the leeward one is in line (on the wind direction) with the rudder post of the upwind one; in Configuration 3 the mast of the leeward model is in line with the rudder post of the upwind one.
The exact position of the Centre of Gravity (CG) of each model is not provided by the manufacturer, so its longitudinal component (Longitudinal Centre of Gravity, LCG) is assumed to be in the same position of the keel's pivot, since the majority of the weight of each model is concentrated in the bulb attached to the tip of the fin keel. The radial distance between the two models is taken between the two pivot points of the models' keels. This distance is kept constant at 800 mm in each configuration. This value corresponds to about 1.3 hull lengths (1.3h in Figure 2). The reason of this choice is to allow enough clearance between the models in Configuration 1. *Table 1* summarizes distances a and b between the CGs of the models.

Table 1:Coordinates of CG of the upwind model with respect to that of the leeward one, for each Configuration and AWA tested

Configuration 1			**Configuration 2**			**Configuration 3**		
AWA	a (mm)	b(mm)	AWA	a (mm)	b(mm)	AWA	a (mm)	b(mm)
25°	338	725	25°	42	799	25°	-320	733
30°	400	693	30°	111	792	30°	-255	758
35°	459	655	35°	180	780	35°	-188	778

When the True Wind Speed (TWS) is constant, the BS changes at different points of sail, i.e. at different True Wind Angles (TWAs). With TWS, TWA and BS, also AWA changes.
The BS is assumed to reach the values of 9, 10.5 and 12 knots at the three AWAs, respectively, in accordance with designers and sailors' experience.
The TWS is set at 13 knots (6.69 m/s). Full scale ACC boats are 80 ft yachts, so the Length Over All (L_{OA}) used for calculations is 24.38 m. The models' L_{OA} is 0.612 m. The length ratio is, therefore:

$$l = \frac{L_{OAm}}{L_{OAs}} = 0.025 \tag{1}$$

Where the subscripts *s* and *m* indicate full scale and model scale, respectively.
Despite Reynolds similitude is more appropriate to scale wind speed, Froude similitude is applied to calculate BS_m, as the former is more impractical to achieve, due to the range of speed chosen and the models' characteristics. BS is therefore scaled according to Equation 2:

$$\frac{BS_s}{\sqrt{g \cdot L_{OAs}}} = \frac{BS_m}{\sqrt{g \cdot L_{OAm}}} \tag{2}$$

Where *g* is the Gravity Acceleration.
The full scale AWS is calculated in accordance with the wind triangle shown in Figure 3.

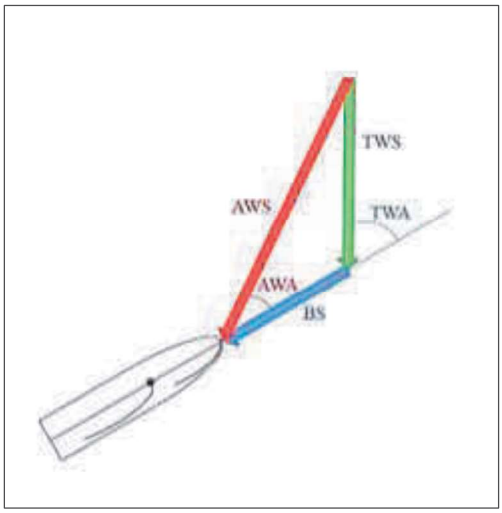

Figure 3: Wind triangle

$$AWS = \frac{BS \cdot \sin\left(\pi - \sin^{-1}\left(\frac{BS}{TWS} \cdot \sin\ AWA\right) - AWA\right)}{\frac{BS}{TWS} \cdot \sin\ AWA} \tag{3}$$

The length of the mainsail's chord in full scale is unknown, hence it is assumed that the sails of the models are built with the same ratio as for the hull and Froude similitude is applied to calculate AWS_m.

$$\frac{AWS_s}{\sqrt{g \cdot C_{mainsail,s}}} = \frac{AWS_m}{\sqrt{g \cdot C_{mainsail,m}}} \tag{4}$$

Where *C* stands for the length of the mainsail's chord at mid-height of mast.
Table 2 shows the calculated values used in the experiments.

Table 2: BS and AWS obtained in Froude similitude

TWS_s (KTS)	**AWA (DEG)**	**BS_s (KTS)**	**BS_s (M/S)**	**AWS_s (KTS)**	**AWS_s (M/S)**	**Fn_{hull}**	**BS_m (M/S)**	**$Fn_{mainsail}$**	**AWS_m (M/S)**
13	25	9	4.63	20.59	10.59	0.3	0.73	1.2	1.68
13	30	10.5	5.40	20.99	10.8	0.45	0.86	1.22	1.71
13	35	12	6.17	20.86	10.73	0.4	0.98	1.21	1.7

2.3. WWC tank setup

The models are set in an upwind leg race scenario, with a heel angle of 25°, the same used by Richards *et al*. [8]. Upright and heeled waterlines are marked on the hulls with the aid of a height gauge, the latter being identified by holding an inclinometer against the mast, while the model is afloat.
Two structures designed on purpose are employed to maintain each model in the right position (heel and AWA) during the WWC Tank tests, as shown in 4. Both the structures are screwed onto a plywood platform, where the positions of the models for the various configurations are marked. The criterion behind the choice of the position on the platform is that both the models should stay as close as possible to the centreline of the tank, in order to minimize the blockage effect of the walls. These positions are drawn in accordance with the coordinates a and b between the CGs described in *Table 1* and to maintain the radial distance of 800 mm. The distances are taken from the centre points of the basis of the two structures.

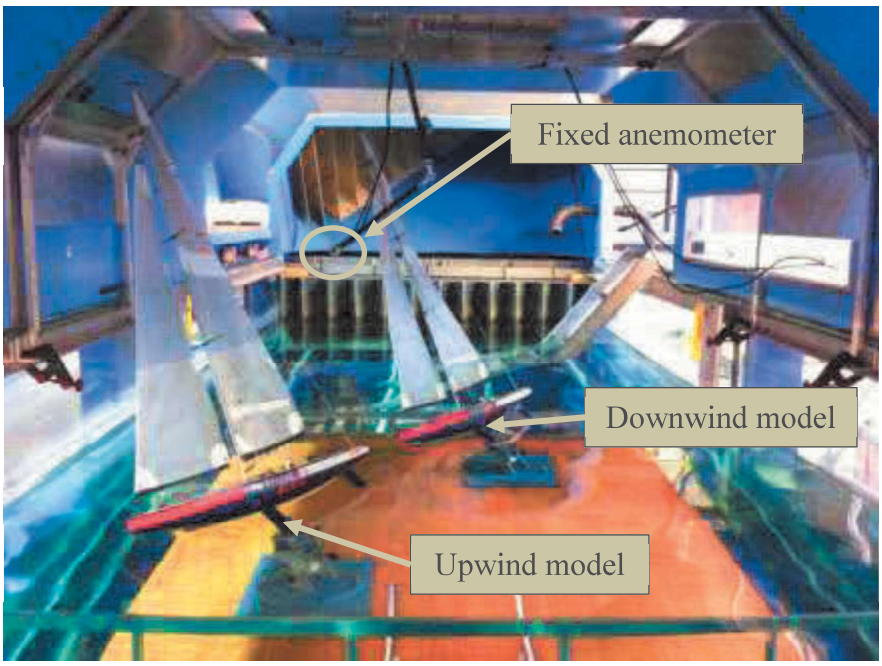

Figure 4: Models in the Wind Wave Current tank

The tank is filled with fresh water until the waterline and the wind is generated by the fan. The sails are trimmed consequently, and the wind intensity is measured. The wind measurements are acquired with two hot wire anemometers: one is placed in a fixed position between the two models, and the other has its sensor on top of a telescopic arm, so it is used to take measurements at the positions that cannot be reached with the first one (Figure). The fixed anemometer is controlled by a software and it is set to measure the wind speed continuously for 35 seconds.

Figure 5: Fixed hot wire anemometer between the two models (left) and telescopic anemometer behind the leeward model (right)

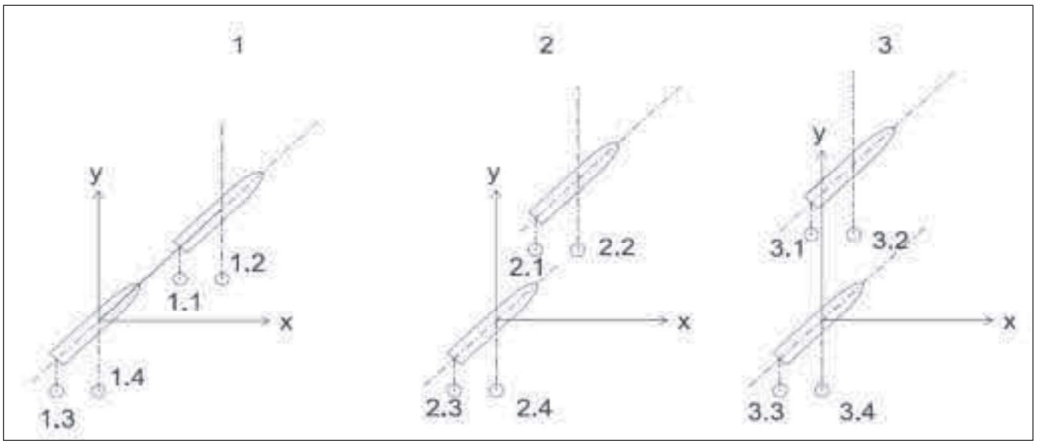

Figure 6: Positions of wind speed measuring point in the Wind Wave Current Tank

Figure describes the position of each measuring point with respect to the LCG of the leeward model for X and Y axis, while Z=0 refers to the waterline. The measure points are named in accordance with their configuration and position, e.g., point 1.1 refers to Configuration 1, position 1; point 1.2 refers to Configuration 1, position 2; etc. For the points *.2, *.3 and *.4, three heights are considered: boom, mid-height of mast and mast head (top). The heights are indicated with the letters b, m and t, respectively. *Table 3*, *Table 4*, *Table 5* provide the coordinates (in mm) of the measuring points.

Table 3: Coordinates of measuring points (mm) for Configuration 1

Configuration 1												
AWA=25°	1.1			1.2			1.3			1.4		
	x	y	z	x	y	z	x	y	z	x	y	z
b				338	363	110	-129	-363	110	0	-363	110
m	209	363	486	338	363	486	-129	-363	486	0	-363	486
t				338	363	862	-129	-363	862	0	-363	862
AWA=30°	1.1			1.2			1.3			1.4		
	x	y	z	x	y	z	x	y	z	x	y	z
b				400	346	110	-153	-346	110	0	-346	110
m	247	346	486	400	346	486	-153	-346	486	0	-346	486
t				400	346	862	-153	-346	862	0	-346	862
AWA=35°	1.1			1.2			1.3			1.4		
	x	y	z	x	y	z	x	y	z	x	y	z
b				459	328	110	-176	-328	110	0	-328	110
m	283	328	486	459	328	486	-176	-328	486	0	-328	486
t				459	328	862	-176	-328	862	0	-328	862

Table 4: Coordinates of measuring points (mm) for Configuration 2

Configuration 2												
AWA=25°	2.1			2.2			2.3			2.4		
	x	y	z	x	y	z	x	y	z	x	y	z
b				42	399	110	-129	-399	110	0	-399	110
m	-88	399	486	42	399	486	-129	-399	486	0	-399	486
t				42	399	862	-129	-399	862	0	-399	862
AWA=30°	2.1			2.2			2.3			2.4		
	x	y	z	`x	y	z	x	y	z	x	y	z
b				111	396	110	-153	-396	110	0	-396	110
m	-42	396	486	111	396	486	-153	-396	486	0	-396	486
t				111	396	862	-153	-396	862	0	-396	862
AWA=35°	2.1			2.2			2.3			2.4		
	x	y	z	x	y	z	x	y	z	x	y	z
b				180	390	110	-176	-390	110	0	-390	110
m	4	390	486	180	390	486	-176	-390	486	0	-390	486
t				180	390	862	-176	-390	862	0	-390	862

Table 5: Coordinates of measuring points (mm) for Configuration 3

Configuration 3												
AWA=25°	3.1			3.2			3.3			3.4		
	x	y	z	x	y	z	x	y	z	x	y	z
b				-320	367	110	-129	-367	110	0	-367	110
m	-449	367	486	-320	367	486	-129	-367	486	0	-367	486
t				-320	367	862	-129	-367	862	0	-367	862
AWA=30°	3.1			3.2			3.3			3.4		
	x	y	z	x	y	z	x	y	z	x	y	z
b				-255	379	110	-153	-379	110	0	-379	110
m	-408	379	486	-255	379	486	-153	-379	486	0	-379	486
t				-255	379	862	-153	-379	862	0	-379	862
AWA=35°	3.1			3.2			3.3			3.4		
	x	y	z	x	y	z	x	y	z	x	y	z
b				-188	389	110	-176	-389	110	0	-389	110
m	-363	389	486	-188	389	486	-176	-389	486	0	-389	486
t				-188	389	862	-176	-389	862	0	-389	862

2.4. Towing tank setup

All three configurations are tested, and three BSs per each. The drag is measured also without the upwind model, in order to compare this result with that of the race configurations. The resistance is measured with the models upright and heeled.
The leeward model is attached to the Gifford dynamometer of the Towing Tank, while the upwind model is attached to a plywood structure that keeps it in the right position, according to Configurations 1, 2 and 3 (Figure).

Figure 7: Plywood structure realised for Towing tank tests

The vertical position of both the models is manually set, in order to have them floating at the correct waterline. In addition, the models are towed with a two-degree leeway.

Since the displacement of the leeward model is not sufficient to balance the weight of the dynamometer, it is necessary to use a counterweight to avoid the model's sinkage. The counterweight is shown in Figure . Its weight is the same as that of the dynamometer: this causes a disturbance in the heave offset for the measurements. It is in fact necessary to adjust it to 0.0 before every run.

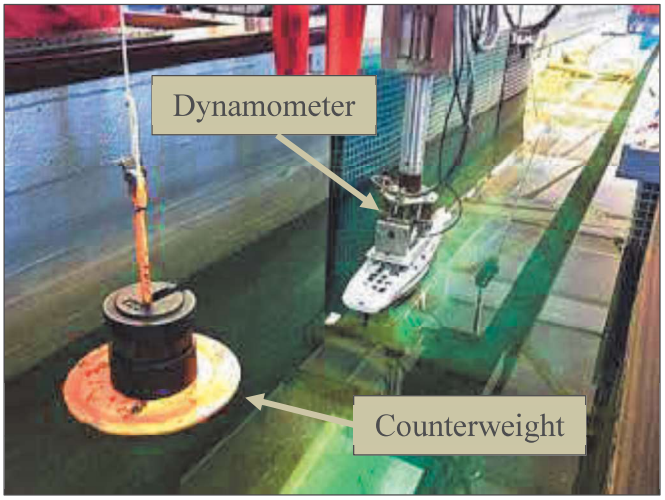

Figure 8: Counterweight mounted behind the dynamometer with a rope-wheel system

2.5. Statistical analysis

The statistical analysis applied to the acquired data has the aim of assessing the reliability of the datasets. A Partial Autocorrelation test is run in order to assess if the sets are composed of independent measures. When an autocorrelation is detected, new samples are extracted from the original sets by selecting every 5th or 10th value. Finally, a two-way ANOVA (Analysis Of Variance) is carried out for the Towing Tank results. The purpose of this analysis is to assess whether speed and configurations (and their combination) affect the hydrodynamic resistance of the towed model.

3. Results and analysis

3.1. Aerodynamics

The fixed hot wire anemometer was set to collect 100 measurements per second, for 35 seconds at each run. The datasets which showed unusual trends (remarkably high fluctuations and small number of point) were pre-processed by removing those trends, symptoms of the great turbulence inside the tanks. An example of this kind of trends is shown in Figure . After this operation, all datasets underwent a Partial Autocorrelation Test, in order to assess whether observations at different time points correlated with one another. The test showed that there was a high correlation between consecutive measurements (correlation coefficient very close to ± 1 for the first lags), meaning that the samples were not composed of independent measurements. Every sample was then filtered, by selecting every 10^{th} measurement. This operation can be carried out because the pursued result is the mean value of the wind speed in a static condition. The so obtained samples had a correlation coefficient of about 0.3for the first lag, which allows to consider it to be composed of independent measurements. Examples of the Partial Autocorrelation Tests are shown in Figure . Both Figure and Figure show data relative to point 1.1m in Configuration 1, at an AWA of 25°.

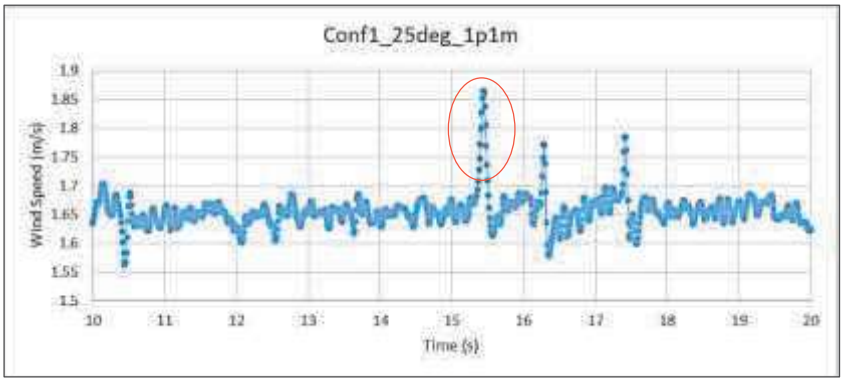

Figure 9: Example of a dataset showing outliers

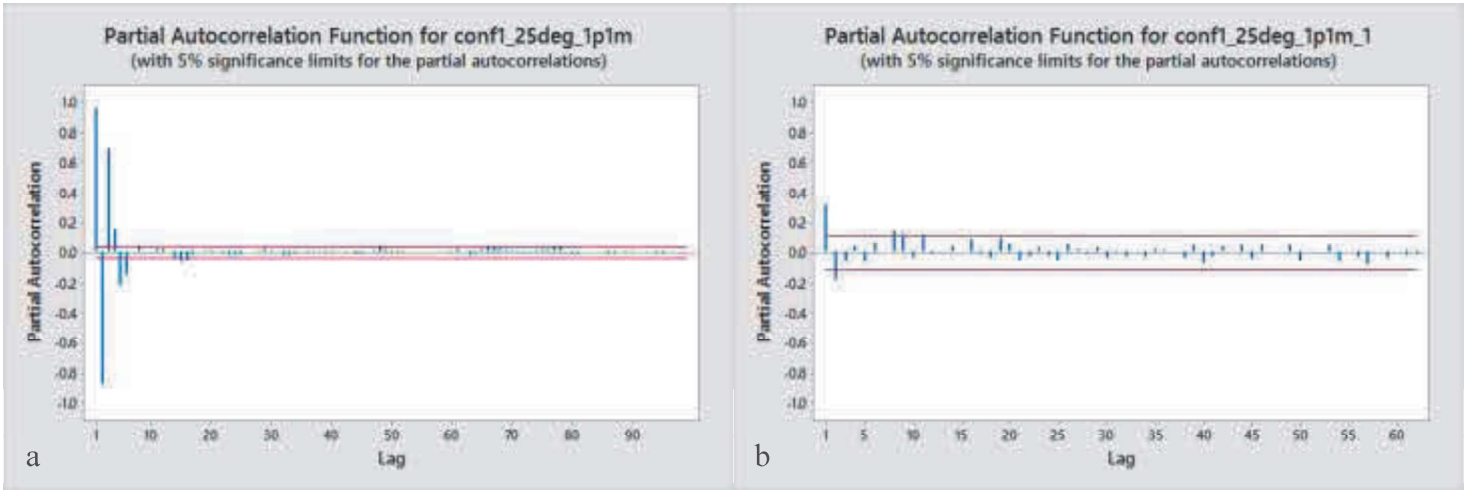

Figure 10: Partial Autocorrelation before (a) and after selecting every 10th measurement (b)

A test for the normality of distribution is then run for all the final datasets, which are all normally distributed around their mean values at a 5% significance level.
The measured values of the wind speed around the two models, and also without the models, for comparison, are shown in **6. Appendix**

Table , in the Appendix. The measurements without the models were taken only with the telescopic anemometer. The standard deviation, hence the turbulence intensity, is available only for sample with a sufficient amount of measurements, i.e. those taken with the fixed anemometer.
Figures 11-13 show the turbulence intensity for points *.1m and *.2b, m, t.

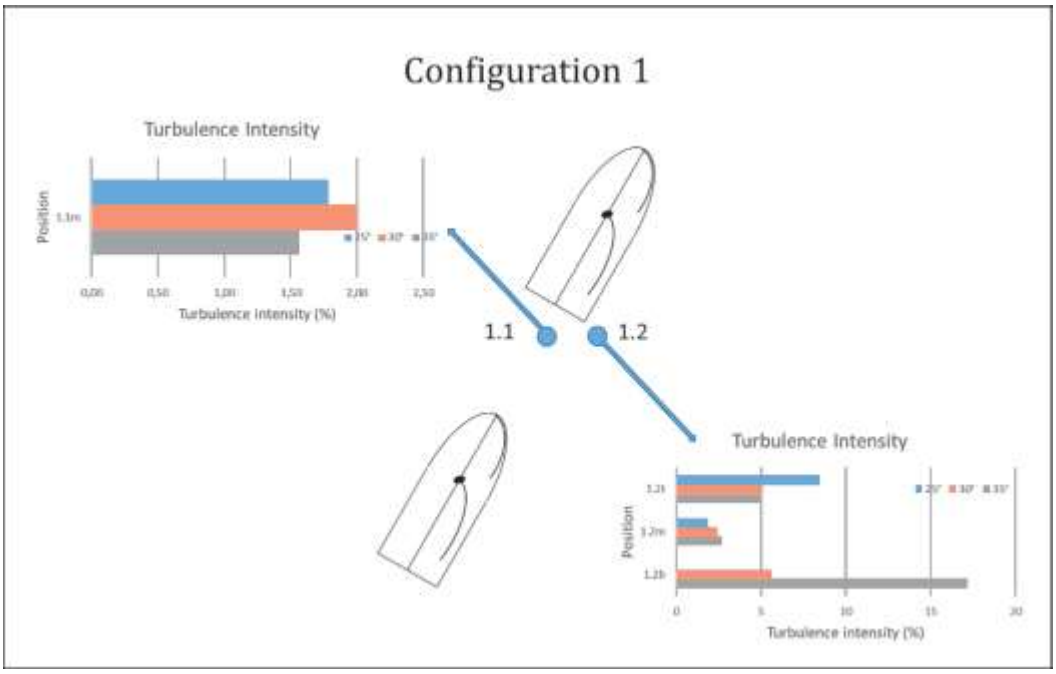

Figure 11: Turbulence intensity in Configuration 1

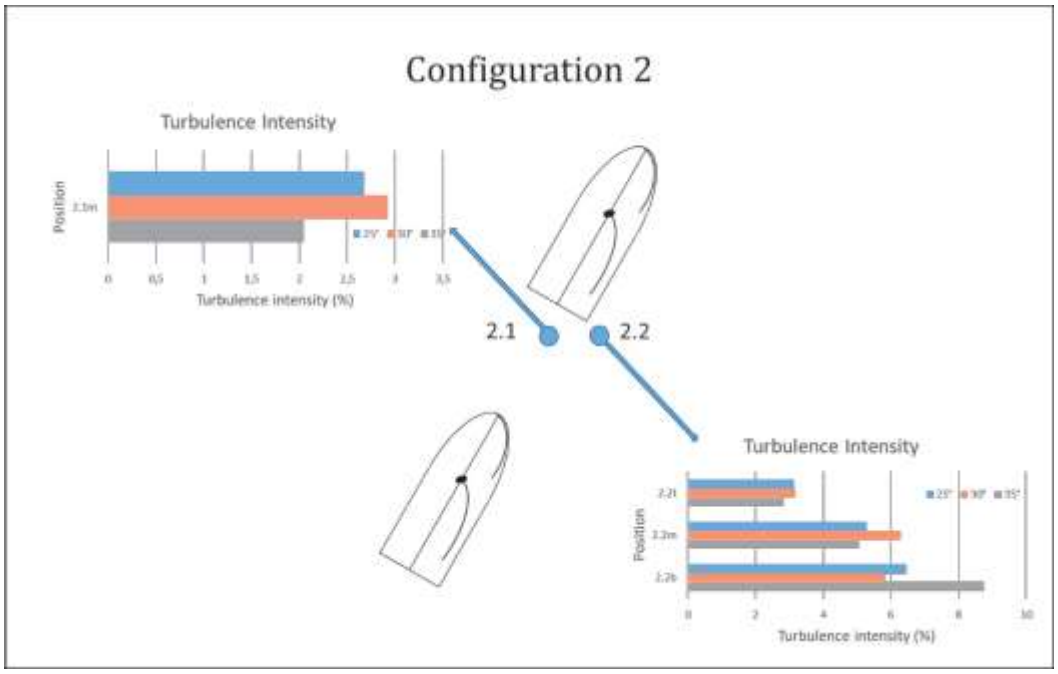

Figure 12: Turbulence intensity in Configuration 2

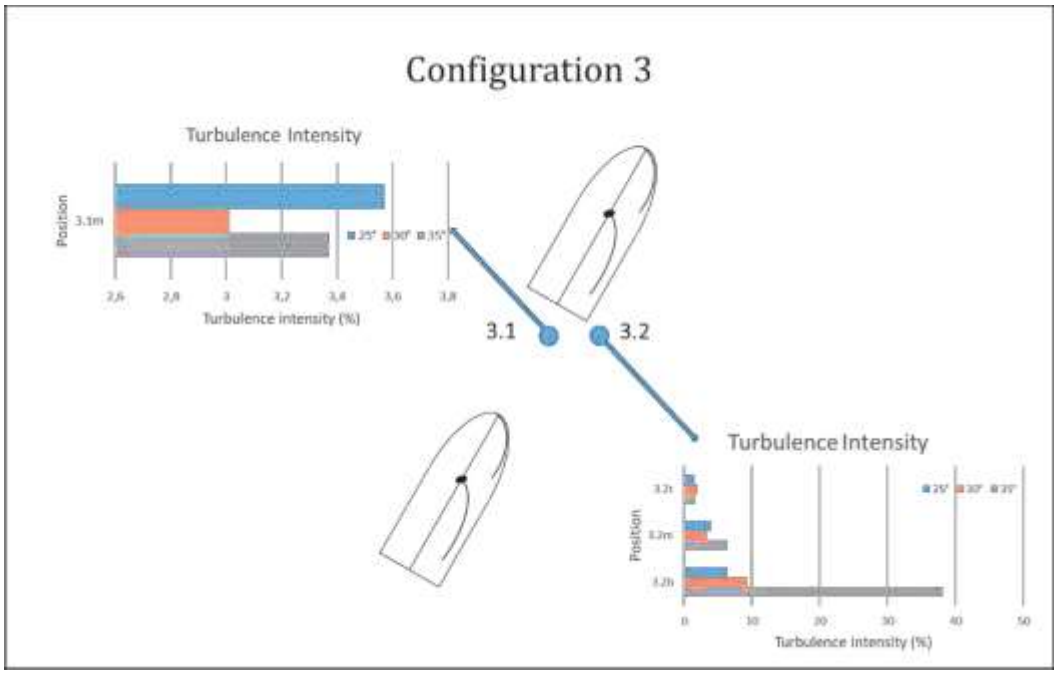

Figure 13: Turbulence intensity in Configuration 3

The wind speed at points *.3b and *.3t could not be measured for all configurations and AWAs, due to the limited availability of the facility: priority was given to the measuring points behind the masts of the models. As far as Configuration 3 is concerned, the wind speed could not be measured at point 3.4t, because of its position. In fact, it was not visible from outside the tank, so it could not be reached with the telescopic anemometer.
For all Configurations and all AWAs, the wind speed changes at different heights from the water surface and at different measure points. However, the wind velocity is expected to increase with the vertical distance from the water surface because of the molecular interactions between the two fluids within the boundary layer. This is not evident from the results presented in 6. Appendix

Table . This discrepancy can be ascribed to the huge turbulence in the WWC Tank. The length of the central measurement section is 3 metres and the models were at its very beginning. This may result in an incident wind flow that is not completely formed, the consequence being a higher amount of turbulence, hence a disturbed measurement. In addition, the models, complete with the sails, reach a height that is excessive for that of the measuring section (see Figure). This translates into a remarkable blockage effect due to the proximity to the tank's walls, which has a negative effect on the data acquiring.
It is possible to notice in Figures 11-13 and in Table 8 that to the area behind the mast of the upwind model, especially at boom height presents a very high turbulence intensity (peak of 38.10%). Here is where a yacht causes the most negative interference and this finding is in accordance with common knowledge among sailors.
In addition, measures of the wind speed were taken at points *.3 and *.4 without the models in the tank, and it is evident that there is an appreciable change, despite the high uncertainty due to the factors described above.
The wind flow appears to be either accelerated or decelerated by the presence of the sails, but a constant pattern is not evident. This can be ascribed to the turbulence and to the small number of measurements taken with the telescopic anemometer.

Nevertheless, it is remarkable that an actual change in the wind speed can be measured in this facility, because it opens the possibility to important developments of this kind of experiments, as described later in the paper.

3.2. Hydrodynamics

The present work is the first attempt of quantification of the changes in the hydrodynamic resistance of a yacht model due to the presence of a second model sailing in close proximity. In addition, towing tanks are designed for testing one vessel at a time, so another important issue to deal with is to design a method to employ two models at once.
Considered the size and weight of the models and the available arrangement for these tests, it is a remarkable outcome to have obtained observable results, even though they are not in total accordance with the expectations. Beneficial improvements for these experiments are further discussed later in the paper.
As for the WWC Tank, a Partial Autocorrelation test was carried out for the measured resistance values. This time, samples with independent measures are obtained by selecting every 5^{th} values from the initial datasets (Partial Autocorrelation coefficient smaller than 0.2). A test for the normality of distribution is then run for all the final datasets, which are all normally distributed around their mean values at a 5% significance level.
A two-way ANOVA is performed on the samples, in order to assess whether there is a statistical relationship between the measured resistance and velocity and configuration, according to the procedure described by Navidi [19]. The results of the ANOVA are presented in *Table* .
For the upright drag, there is a strong evidence in favour of the null hypothesis that the additive method is plausible for this dataset, i.e. the interactions between the two factors velocity and configuration are 0. This is shown by the P-value being greater than 0.1 for the source configuration*velocity. In addition, the low P-values for the other sources show that the drag depends upon both the velocity and the configuration.
For the heeled drag, the P-Value describing the interaction between velocity and configuration is smaller than 0.1, but still greater than 0.05; this means that the evidence against the null hypothesis is slight, so the additive method can be considered plausible also in this case. In this case, the configurations seem not to affect the changes in the resistance, since the P-value is very high. On the other hand, the P-Value 0 shows that the drag is again dependent on the velocity, in accordance with the expectation.

Table 6: Results of the two-way ANOVA for upright and heeled resistance

Upright resistance		**Heeled resistance**	
Source	P-Value	Source	P-Value
Velocity	0.000	Velocity	0.000
Configuration	0.018	Configuration	0.147
Configuration*Velocity	0.479	Configuration*Velocity	0.065

It is common practice to describe the resistance of a model with non-dimensional coefficients, however in this work it is presented as a force (expressed in Newton), because neither the wetted surface (S) nor the Waterline Length (L_{WL}) of the models are known. Measuring the L_{WL} would bring more uncertainty to the result, which is already affected by the background noise. The same situation applies to the Displaced Volume (Δ), that can be easily calculated, but the presence of the counterweight makes it necessary to adjust the heave offset before every run. Therefore, this may affect the results as well.

Table 7: Average and standard deviation values of the resistance measured in the Towing Tank

Configuration	Velocity (m/s)	Average resistance (N)	Standard deviation (N)
Single upright	0.73	0.18	0.76
Single upright	0.86	0.44	0.90
Single upright	0.98	0.59	1.02
Single heeled	0.73	0.22	1.01
Single heeled	0.86	0.37	1.11
Single heeled	0.98	0.76	1.29
1 upright	0.73	0.16	0.86
1 upright	0.86	0.3	0.96
1 upright	0.98	0.36	1.00
1 heeled	0.73	0.20	1.01
1 heeled	0.86	0.33	1.01
1 heeled	0.98	0.48	1.15
2 upright	0.73	0.34	0.96
2 upright	0.86	0.39	0.92
2 upright	0.98	0.52	1.18
2 heeled	0.73	0.3	0.92
2 heeled	0.86	0.32	1.10
2 heeled	0.98	0.38	1.21
3 upright	0.73	0.18	0.91
3 upright	0.86	0.41	0.91
3 upright	0.98	0.43	1.15
3 heeled	0.73	0.30	1.06
3 heeled	0.86	0.30	1.18
3 heeled	0.98	0.61	1.34

The measured resistance grows with the towing speed, as expected.
As suggested by the ANOVA, the different configurations seem to have a noticeable effect on the measured resistance. In particular, it is evident that Configuration 1 brings a positive effect in both upright and heeled cases, as the resistance of the leeward model is always smaller than that of the single hull. This result is in accordance with expectations, as the vortexes generated by the separation of the boundary layer behind the upwind model create a depression, which translates into a decrease in the hydrodynamic resistance of the leeward model.
Configuration 2 appears to have a negative effect at low speed, while it allows the resistance to decrease when the speed grows. This behaviour is observed when the models are both upright and heeled.
When the models are towed upright, Configuration 3 has a slight negative effect at low speed, while it generates a positive interaction at higher speeds. On the other hand, with heeled models the resistance in Configuration 3 is considerably greater than that of the single hull at low speed, but it is smaller at higher speeds.
It is interesting to notice that the highest value of heeled resistance (a yacht would not be likely to sail upwind in an upright position) occurs for Configuration 3, 0.98 m/s, i.e. AWA=35°. This corresponds to the situation where the leeward model encounters the most intense turbulence, due to the aerodynamic interference between the sails.

However, the reliability of the observed data is questionable, for the standard deviation of all the samples is relatively high, as shown in *Table* . This is a consequence of the intense background noise.

The results obtained are not always completely satisfactory, but they show that it is possible to arrange experiments with two models in a towing tank. This result opens up a wide range of opportunities for researchers, since it proves that investigations of hydrodynamic interactions are accomplishable in a towing tank.

In addition, aerodynamic tests can be substantially improved by carrying them out in a WWC Tank, since it offers a great advantage compared to a wind tunnel: the presence of both air and water. In this work, the models have 0 DoF in the test setup, but a different arrangement that allows them to move freely would ensure a more realistic response, which could lead to a more accurate interaction model. Also the dynamic nature of the aerodynamic interactions could be measured, producing even more realistic results.
In conclusion, further research with this combination of facilities is possible and has the potential to produce remarkable results. It should be carried out with adequate resources, which can easily overcome the difficulties and problems outlined in this paper.

4. Conclusions and recommendations for further development

This paper presented an experimental study of the physical interactions between two yachts sailing in proximity. For the first time, an attempt at measuring both aero and hydrodynamic interactions was made using a towing tank and a wind wave and current tank at Newcastle University. A novel setup was developed to accommodate two models in the facilities, and to measure wind in different points. The experiments highlighted some challenges and limitations related to the facilities used, and the main findings shown in the paper, and recommendation for future work are as follows:

- The measuring section size of the WWC Tank is small compared to the size of the models, with the result being the inaccuracy of the measurements, due to the high blockage effect of the tank's walls. The models, though, should not be smaller, otherwise it would be even more difficult to obtain a measurable change in the wind speed around the sails;
- The telescopic anemometer is not as accurate as the fixed one, because it has to be held in position manually, so having only fixed hot wire anemometers would improve the quality of data and make the measuring process faster;
- The anemometers themselves should affect the measurements as little as possible, so the structures holding them should be as aerodynamic as possible;
- A model tested in a towing tank should provide enough displacement to support the dynamometer. This would result in the absence of the counterweight, whose inertia may bias the measures;
- A heavier, hence bigger, model would be steadier during the carriage run, so its yaw would decrease. This would result in a better response from the dynamometer's load cell, since the starboard and portside sensor's measures would not be affected by the excessive horizontal vibration of the model.

The results show it is possible to achieve the desired measurements in these facilities, although improvements are necessary. Aerodynamic tests show a higher turbulence in the area behind the lower part of the model's mast, which is in accordance with the expectations. The hydrodynamic tests are remarkable as they show that differences in the interactions between hulls are observable, according to their different relative positions.

5. References

1. Claughton, A., J. Wellicome, and A. Shenoi, *Sailing Yacht Design Theory*. 2006.
2. Fossati, F., ed. *Aero-hydrodynamics and the Performance of Sailing Yachts*. 2009.
3. Marchaj, C.A., *Aero-hydrodynamics of sailing*. Rev. and expanded ed.. ed. 1988, Camden, Me.: Camden, Me. : International Marine Publishing.
4. Gerritsma, J., R. Onnink, and A. Versluis, *Geometry, resistance and stability of the Delft systematic yacht hull series.* International Shipbuilding Progress, 1981. **28**(328): p. 276-286.
5. Keuning, J.A. and U.B. Sonnenberg, *Approximation of the Hydrodynamic Forces on a Sailing Yacht based on the Delft Systematic Yacht Hull Series.* 1998.
6. Milgram, J.H., D.B. Peters, and D.N. Eckhouse, *Modeling IACC sail forces by combining measurements with CFD*, in *The eleventh Chesapeake sailing yacht smposium*. 1993.
7. Schlageter, E.C. and J.R. Teeters, *Performance Prediction Software for IACC Yachts*, in *The eleventh Chesapeake sailing yacht symposium*. 1993.
8. Richards, P.J., et al., *A wind tunnel study of the interactions between two sailing yachts*, in *The 21st Chesapeake sailing yacht symposium*. 2013.
9. Aubin, N., *Wind tunnel modeling of aerodynamic interference in a fleet race*. 2013, Université de Nantes.
10. Spenkuch, T., et al., *Modelling multiple yacht sailing interactions between upwind sailing yachts.* Journal of Marine Science and Technology, 2011. **16**(2): p. 115-128.
11. Philpott, A.B., S.G. Henderson, and D. Teirney, *A simulation model for predicting yacht match race outcome.* Operations research, 2004. **52**: p. 1-16.
12. Tagliaferri, F., et al., *On risk attitude and optimal yacht racing tactics.* Ocean Engineering, 2014. **90**: p. 149-154.
13. Tagliaferri, F., I.M. Viola, and R.G.J. Flay, *Wind direction forecasting with artificial neural networks and support vector machines.* Ocean Engineering, 2015. **97**: p. 65-73.
14. Jacquin, E., et al., *Toward numerical VPP with the full coupling of hydrodynamic and aerodynamic solvers for ACC yacht*, in *The 17th Chesapeake sailing yacht symposium*. 2005. p. 1-12.
15. Marino, A., *Aerodynamic and Hydrodynamic Interactions between two Yachts Sailing Upwind*, in *School of Marine Science and Technology*. 2016, Newcastle University.
16. ncl.ac.uk. 2016 5th August 2016]; Available from: http://www.ncl.ac.uk/marine/facilities/hydrodynamics/#about.
17. kyosho.com. 2016 2nd July 2016]; Available from: http://www.kyosho.com/eng/products/rc/detail.html?product_id=109866.
18. Cup, A.s. *History of the America's Cup*. [cited 2017 12th July]; Available from: https://www.americascup.com/en/history.html.
19. Navidi, W.C., *Statistics for engineers and scientists*. 3rd ed.. ed. 2011, New York: New York : McGraw-Hill.

6. Appendix

Table 8: Wind speed measured with fixed and telescopic anemometers

Configuration	AWA (deg)	Point	AWS-mean (m/s)	AWS-standard deviation (m/s)	Turbulence intensity (%)	AWS-mean without models (m/s)
1	25°	1.1m	1.5	0.03	1.78	
1	25°	1.2b	1.83			
1	25°	1.2m	1.55	0.03	1.84	
1	25°	1.2t	1.4	0.12	8.43	
1	25°	1.3b	1.89			1.90
1	25°	1.3m	1.81			1.83
1	25°	1.3t	1.79			1.80
1	25°	1.4b	1.63			1.92
1	25°	1.4m	1.88			1.79
1	25°	1.4t	1.82			1.80
1	30°	1.1m	1.69	0.03	2.00	
1	30°	1.2b	1.99	0.11	5.59	
1	30°	1.2m	1.93	0.05	2.40	
1	30°	1.2t	1.70	0.09	5.04	
1	30°	1.3b	2.11			2.15
1	30°	1.3m	2.07			2.05
1	30°	1.3t	2.14			2.05
1	30°	1.4b	1.72			2.15
1	30°	1.4m	1.98			2.06
1	30°	1.4t	1.90			2.23
1	35°	1.1m	1.73	0.03	1.56	
1	35°	1.2b	1.92	0.33	17.10	
1	35°	1.2m	1.81	0.05	2.66	
1	35°	1.2t	1.59	0.08	4.91	
1	35°	1.3b	2.12			2.09
1	35°	1.3m	2.04			1.99
1	35°	1.3t	2.05			1.97
1	35°	1.4b	0.48			2.05
1	35°	1.4m	1.85			1.98
1	35°	1.4t	2.00			2.06
2	25°	2.1m	1.54	0.04	2.67	
2	25°	2.2b	2.16	0.14	6.45	
2	25°	2.2m	1.46	0.08	5.28	
2	25°	2.2t	1.57	0.05	3.13	
2	25°	2.3m	1.88			1.83
2	25°	2.4b	1.84			1.80
2	25°	2.4m	1.63			1.79
2	25°	2.4t	1.82			1.80
2	30°	2.1m	1.84	0.05	2.92	
2	30°	2.2b	2.29	0.13	5.81	
2	30°	2.2m	1.73	0.11	6.28	
2	30°	2.2t	1.88	0.06	3.16	
2	30°	2.3m	2.06			2.05
2	30°	2.4b	2.07			2.15
2	30°	2.4m	1.86			2.06
2	30°	2.4t	2.04			2.23
2	35°	2.1m	1.86	0.04	2.04	
2	35°	2.2b	2.51	0.22	8.77	

Configuration	AWA (deg)	Point	AWS-mean (m/s)	AWS-standard deviation (m/s)	Turbulence intensity (%)	AWS-mean without models (m/s)
2	35°	2.2m	1.73	0.09	5.06	
2	35°	2.2t	1.80	0.05	2.82	
2	35°	2.3b	2.03			
2	35°	2.3m	2.07			1.99
2	35°	2.3t	1.98			
2	35°	2.4b	1.47			2.05
2	35°	2.4m	1.76			1.98
2	35°	2.4t	2.01			2.06
3	25°	3.1m	1.51	0.05	3.57	
3	25°	3.2b	2.02	0.13	6.33	
3	25°	3.2m	1.57	0.06	3.91	
3	25°	3.2t	1.52	0.02	1.48	
3	25°	3.3m	1.66			1.83
3	25°	3.4b	1.71			1.86
3	25°	3.4m	1.82			1.80
3	30°	3.1m	1.82	0.055	3.01	
3	30°	3.2b	2.1	0.19	9.16	
3	30°	3.2m	1.73	0.06	3.30	
3	30°	3.2t	1.77	0.03	1.92	
3	30°	3.3m	2.02			2.02
3	30°	3.4b	2.04			2.02
3	30°	3.4m	2.05			1.97
3	35°	3.1m	1.8	0.06	3.37	
3	35°	3.2b	1.05	0.4	38.10	
3	35°	3.2m	1.7	0.11	6.37	
3	35°	3.2t	1.65	0.03	1.56	
3	35°	3.3m	1.65			2.01
3	35°	3.4b	1.93			2.01
3	35°	3.4m	1.93			1.91